Polar Geosci., **12**, 49–70, 1999

PETROLOGY AND METAMORPHISM OF SAPPHIRINE-BEARING ALUMINOUS GNEISSES FROM TONAGH ISLAND IN THE NAPIER COMPLEX, EAST ANTARCTICA

Tomokazu HOKADA[1], Yasuhito OSANAI[2], Tsuyoshi TOYOSHIMA[3], Masaaki OWADA[4], Toshiaki TSUNOGAE[5] and Warwick A. CROWE[6]

[1]*Department of Polar Science, School of Mathematical and Physical Sciences, The Graduate University for Advanced Studies, Kaga 1-chome, Itabashi-ku, Tokyo 173-8515*
[2]*Department of Earth Sciences, Faculty of Education, Okayama University, Tsushima-naka 3-chome, Okayama 700-8530*
[3]*Graduate School of Science and Technology, Niigata University, Ikarashi 2-chome, Niigata 950-2181*
[4]*Department of Earth Sciences, Faculty of Science, Yamaguchi University, Yoshida 1677–1, Yamaguchi 753-8512*
[5]*Faculty of Education, Shimane University, Nishi Kawatsu, Matsue 690-8504*
[6]*Department of Geology and Geophysics, University of Western Australia, Nedlands, Perth, WA 6907, Australia*

Abstract: A variety of Mg-rich silica-undersaturated aluminous gneisses containing sapphirine, spinel and corundum occur within the ultrahigh-temperature (UHT) metamorphic sequence at Tonagh Island in the Napier Complex, East Antarctica. They occur as blocks or pods in quartzo-feldspathic gneisses or mafic granulite, or as thin layers around ultramafic rocks. The modes of occurrence, constituent minerals and mineral textures of these aluminous gneisses are different from each other, suggesting that they are derived from different protoliths or formation processes. Field occurrences suggest that some of the aluminous gneisses on Tonagh Island may not be simple pelitic precursors but were formed through processes associated with partial melting or metasomatism. Various reaction textures and compositional zoning in constituent minerals, which reflect retrograde metamorphism, are commonly observed in these rocks. Garnet-orthopyroxene geothermobarometry using the chemical compositions of the cores of garnet and orthopyroxene yields slightly lower temperatures (800–1000°C at 0.5–1.0 GPa) than the thermal climax (1100°C). Pressure condition of 0.8–1.1 GPa at the thermal peak (1030–1100°C) is estimated from the garnet-orthopyroxene geobarometry.

key words: Aluminous gneiss, Napier Complex, Sapphirine, Tonagh Island, ultrahigh-temperature metamorphism

1. Introduction

The Napier Complex in Enderby Land, East Antarctica, is one of the oldest complexes in the world with initial felsic igneous activity of 3.8 Ga and major metamorphic events older than 2.5 Ga (HARLEY and BLACK, 1997; and see references therein). It is also known as having undergone extremely high temperature metamorphism, called ultrahigh-temperature (UHT) metamorphism (SPEAR, 1993; HARLEY, 1998), characterized

by mineral parageneses including sapphirine+quartz (DALLWITZ, 1968; ELLIS *et al.*, 1980; GREW, 1980, 1982; MOTOYOSHI and MATSUEDA, 1984; MOTOYOSHI and HENSEN, 1989), osumilite (ELLIS *et al.*, 1980; GREW, 1982; MOTOYOSHI and MATSUEDA, 1984; HENSEN and MOTOYOSHI, 1992), and inverted metamorphic pigeonite (SANDIFORD and POWELL, 1986, 1988; HARLEY, 1987).

The occurrence of sapphirine, either coexisting with quartz or not, is restricted to magnesian or aluminous rocks, and is not common in the Napier Complex. Several papers have reported the occurrence of sapphirine-bearing gneisses from the Napier Complex; they include petrological studies with textural and electron microprobe analysis (ELLIS *et al.*, 1980; GREW, 1980, 1982; MOTOYOSHI and MATSUEDA, 1984; HARLEY, 1985, 1986; SHERATON *et al.*, 1987; MOTOYOSHI and HENSEN, 1989; HENSEN and MOTOYOSHI, 1992) and descriptions of the mineral assemblages only (DALLWITZ, 1968; SHERATON *et al.*, 1980; SANDIFORD, 1985; MAKIMOTO *et al.*, 1989; ISHIZUKA *et al.*, 1998). The protoliths of these sapphirine-bearing gneisses are generally regarded as pelitic precursors, but little description has been given of the field occurrences of these distinctive rocks, especially of the geological relationship to the surrounding rocks.

Sapphirine-bearing aluminous gneisses occur at several localities on Tonagh Island and display at least three different modes of occurrence, *i.e.*, 1) thin layers around ultramafic rock, 2) block in the alternation of quartzo-feldspathic gneiss and mafic granulite, and 3) block surrounded by leucocratic quartzo-feldspathic gneiss. The field occurrences in our survey suggest that some of the aluminous gneisses on Tonagh Island may not be simple pelitic precursors but formed through the processes associated with partial melting or metasomatism. This paper reports the field occurrences, petrography and mineral

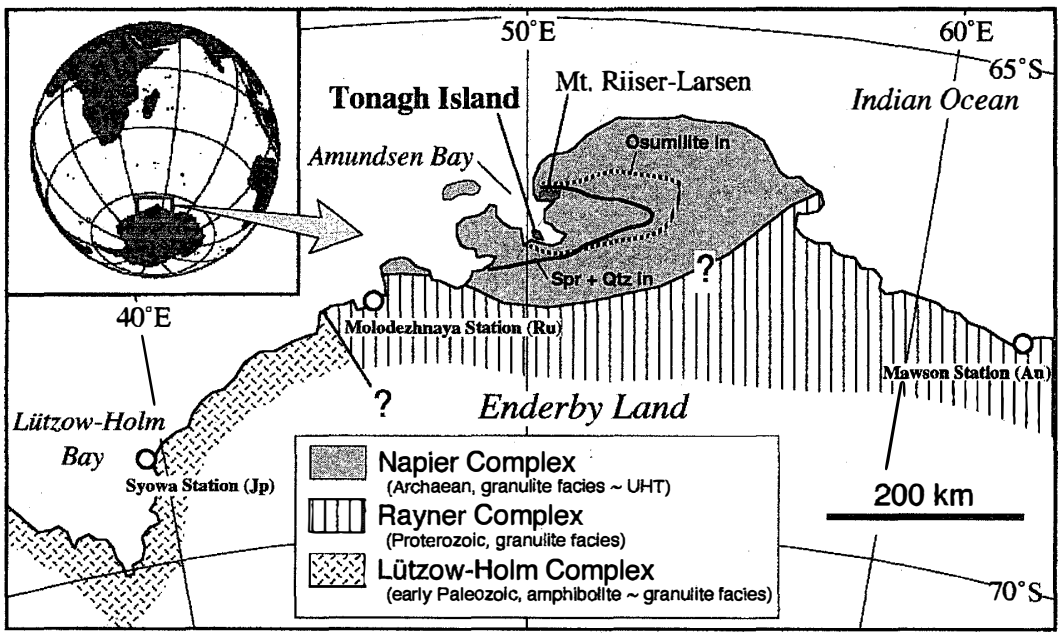

Fig. 1. Geological outline involving the Napier Complex and the surrounding areas including the locality of Tonagh Island. The estimated boundary between the Napier Complex and the Rayner Complex is after SHERATON et al. (1987). Isograds of 'sapphirine (Spr)+quartz (Qtz) in' and 'osumilite in' of the Napier Complex are after HARLEY and HENSEN (1990).

chemistry of the sapphirine-bearing aluminous gneisses from the northern part of the island (Units I and II), and gives a brief discussion of the metamorphism of the area.

2. Field Occurrence and Petrography

The Napier Complex is composed mainly of quartzo-feldspathic gneisses with minor amounts of mafic granulite, garnet gneiss, garnet-sillimanite gneiss, garnet-orthopyroxene gneiss, sapphirine-bearing aluminous gneisses, impure quartzite, magnetite-quartz gneiss and ultramafic rocks (SHERATON *et al.*, 1987). HARLEY and HENSEN (1990) summarized the regional metamorphism of the complex, and described a the high-grade region, where the mineral parageneses of sapphirine+quartz and osumilite occur, around Amundsen Bay (Fig. 1).

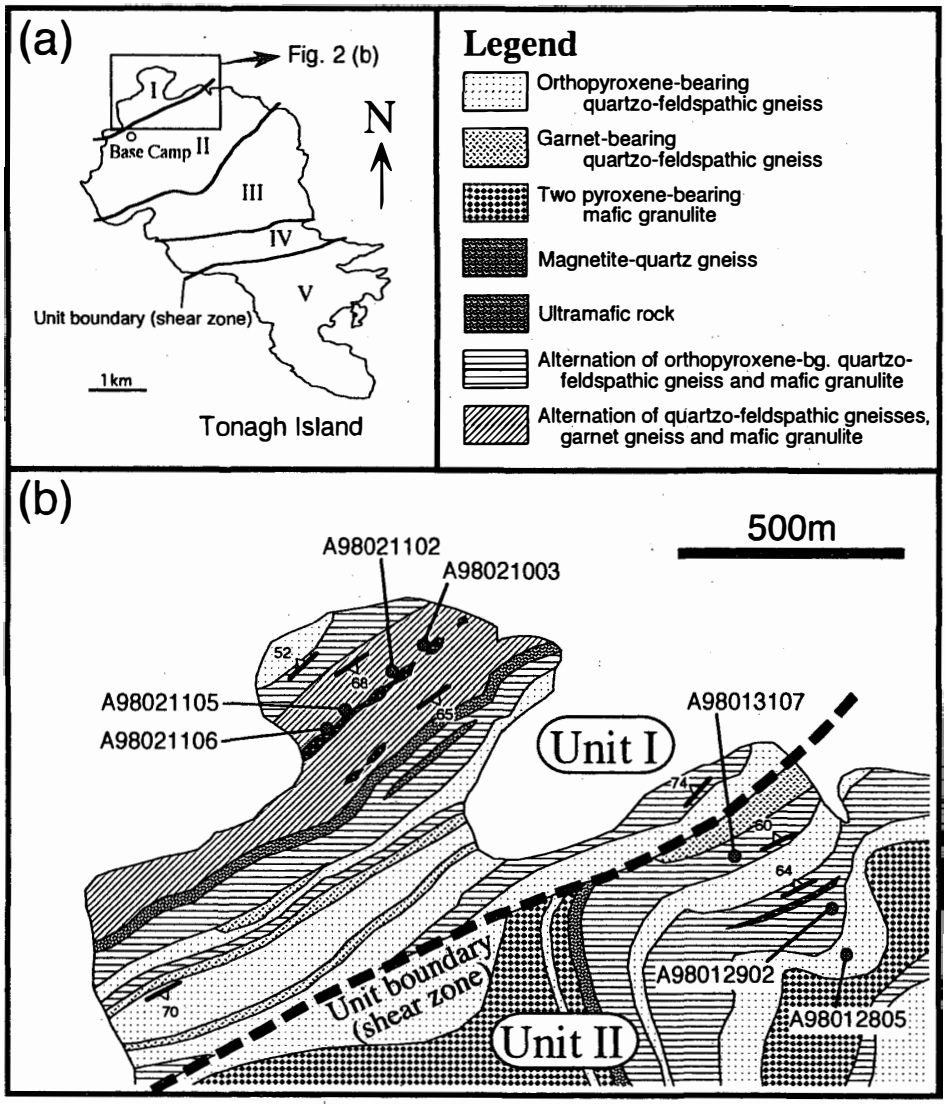

Fig. 2. Geological map of Tonagh Island (northern part). (a) Distributions of pseudotachylite- and mylonite-bearing shear zones which divide geological units (I, II, III, IV and V). (b) Geological map of the northern part of Tonagh Island, and the sample localities of sapphirine-bearing aluminous gneisses described in the text.

Table 1. Constituent minerals and their chemical features in the aluminous gneisses. Mineral abbreviations are as follows. Spr: sapphirine, Opx: orthopyroxene, Grt: garnet, Spl: spinel, Phl: phlogopite, Sil: sillimanite, Crn: corundum, Crd: cordierite, Pl: plagioclase, Akfs: alkali feldspar, Qtz: quartz. Rutile, ilmenite, biotite, zircon and monazite are accessory phases.

												Spr			Opx		Grt				Spl		Phl	
sample	Spr	Opx	Grt	Spl	Phl	Sil	Crn	Crd	Pl	Akfs	Qtz	X_{Mg} min	Al_2O_3 min	Cr_2O_3 max	X_{Mg} *	Al_2O_3 max	X_{Mg} max	*alm*	*prp*	*grs*	X_{Mg} max	ZnO max	X_{Mg} min	F max
A98021106A	○	○	○			○			○	○		0.79	58.6	2.2	0.76	7.7	0.57	*0.42*	*0.55*	*0.02*				
A98021105A	○	○	○			○		○	○			0.84	61.6	0.1	0.79	10.4	0.62	*0.37*	*0.60*	*0.03*				
A98021102H	○	○	○	○			○		○	○		0.80	60.2	0.8	0.75	8.6	0.52	*0.46*	*0.50*	*0.03*	0.56	0.2		
A98021003E	○	○	○						○	○		0.80	61.2	0.7	0.78	8.5	0.63	*0.36*	*0.59*	*0.04*				
A98013107A	○			○	○		○		○			0.82	64.2	0.1							0.49	1.1	0.90	5.5
A98013107C	○			○	○		○	○	○			0.93	64.1	0.0							0.81	0.3	0.96	5.3
A98012902D	○	○	○						○			0.77	59.6	0.1	0.74	10.6	0.53	*0.46*	*0.52*	*0.01*				
A98012902I	○	○	○	○		○	○		○			0.76	61.4	0.1	0.69	9.3	0.53	*0.46*	*0.52*	*0.01*	0.56	1.0		
A98012902J	○	○	○						○			0.81	62.3	0.1	0.71	10.3	0.56	*0.43*	*0.55*	*0.01*				
A98012902P		○	○	○		○	○		○		(Δ)				0.69	9.2	0.52	*0.47*	*0.51*	*0.01*	0.65	1.1		
A98012805B	○	○	○	○		○	○		○	(Δ)	(Δ)	0.79	61.0	0.1	0.70	9.5	0.51	*0.48*	*0.49*	*0.02*	0.62	16.1		

○ : present (Δ) : local

X_{Mg} = Mg/(Mg+Fe) Al_2O_3, Cr_2O_3, ZnO, F : wt.% * : value at max Al_2O_3

Tonagh Island is located in the Amundsen Bay region, the high-grade part of the Napier Complex (Fig. 1). Mylonite and pseudotachylite-bearing shear zones divide the island into five units (Fig. 2). The central (Units II and III) and the southern (Units IV and V) parts of the island are composed mainly of the alternation (several meters order) of quartzo-feldspathic gneiss and mafic granulite, and that of orthopyroxene-bearing and garnet-bearing quartzo-feldspathic gneisses, respectively. On the other hand, in the northernmost part (Unit I), centimeter to meter order alternation of orthopyroxene and garnet-bearing quartzo-feldspathic gneisses, two-pyroxene mafic granulite, garnet gneiss, garnet-sillimanite gneiss, garnet-orthopyroxene gneiss, sapphirine-bearing aluminous gneiss, magnetite-quartz gneiss, pyroxenite and ultramafic rock are developed. A detailed geological outline of Tonagh Island is described in OSANAI *et al.* (1999, in this volume). The aluminous gneisses occur as blocks or pods in quartzo-feldspathic gneisses or mafic granulite, or as thin layers around ultramafic rocks.

Sample localities of the aluminous gneisses described in this paper are shown in Fig. 2. Table 1 summarizes the constituent minerals and their chemical features.

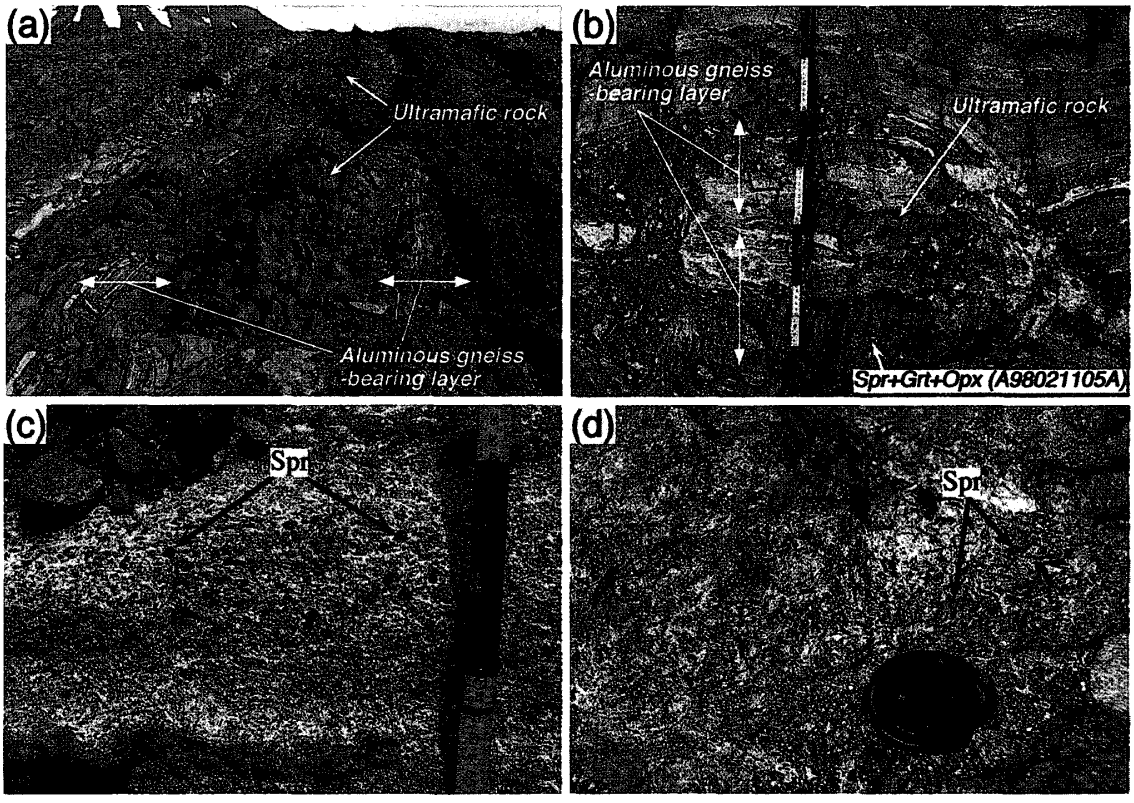

Fig. 3. Sapphirine-bearing aluminous gneiss layer around ultramafic rock in Unit I. (a) Boudinaged ultramafic layer accompanying sapphirine-bearing gneisses in the centimeter to meter order alternation of quartzo-feldspathic gneisses, mafic granulite, garnet gneiss, garnet-sillimanite gneiss, magnetite-quartz gneiss and pyroxenite. (b) Boudinaged ultramafic rock and surrounding feldspathic and aluminous gneisses. Garnet and orthopyroxene with minor sapphirine concentrate on the lower part of the photograph (A98021105). Leucocratic feldspathic vein develops at the boudin neck. (c) Garnet-bearing feldspathic portion in the aluminous layer (A98021106). Porphyroblastic sapphirine occurs and is accompanied by fine-grained orthopyroxene. (d) Idiomorphic sapphirine-rich portion (A98021003).

2.1. Sapphirine-garnet-orthopyroxene gneiss (A98021106A, A98021105A, A98021102H, A98021003E)

This occurs as a several centimeters to a few meters thick layer around an ultramafic layer, which is locally boudinaged or shows pinch-and-swell structure, in the alternation zone of the northwest peninsula of the island (Fig. 3a). This layer crops out intermittently over 400 m along the strike. Mineral assemblages and modal proportions of constituent minerals are heterogeneous, and leucocratic feldspathic veins occasionally develop at the boudin neck or among the boudinaged ultramafic layer and surrounding aluminous gneisses. Representative lithologies are as follows:

A98021106A: Feldspathic portion containing garnet and sapphirine (Figs. 3c and 4a). Garnet is generally rounded. Sapphirine is porphyroblastic up to a few mm in diameter, and has exsolution lamellae of rutile and quartz. Xenomorphic and relatively fine-grained (less than 1 mm) orthopyroxene occasionally occur around sapphirine. The matrix of the gneiss is composed of plagioclase (antiperthite) and alkali feldspar (perthite-mesoperthite). Quartz is not present.

A98021105A: Garnet and orthopyroxene-rich portion with minor amounts of

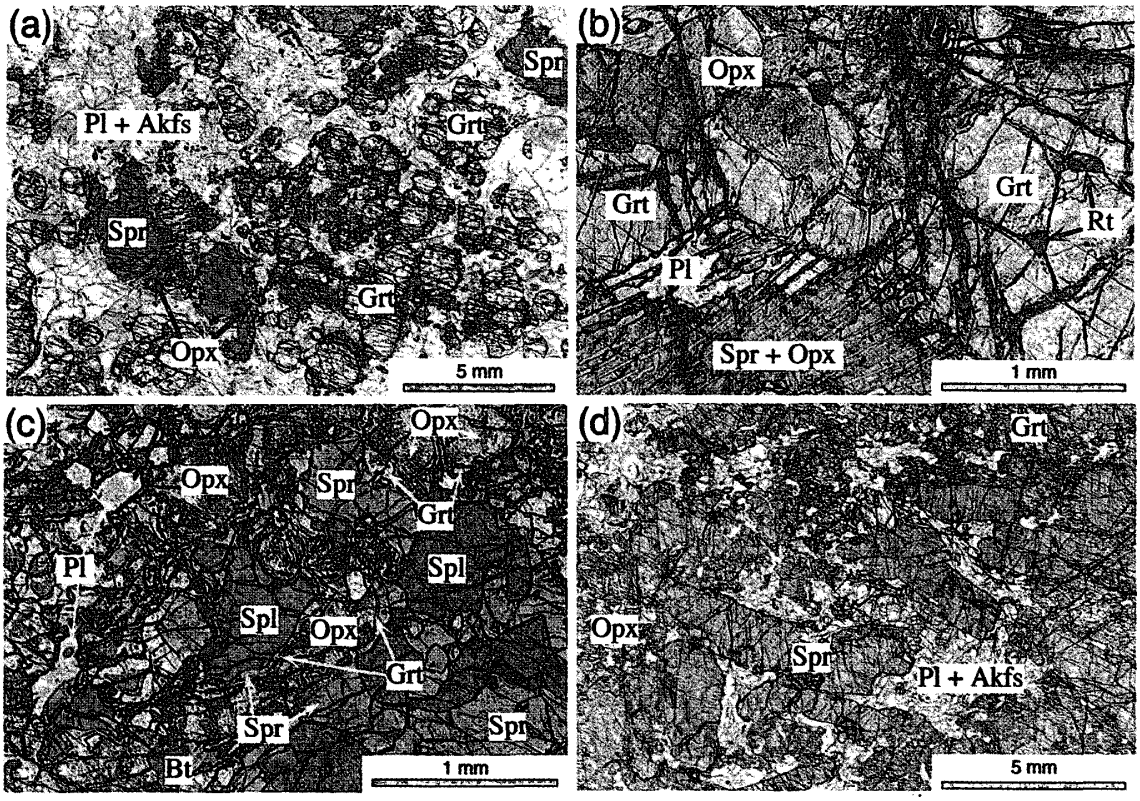

Fig. 4. Photomicrograph of sapphirine-bearing aluminous gneisses in Unit I. Plane-polarized light. (a) A98021106A: Porphyroblastic sapphirine and rounded garnet occur in the matrix of plagioclase (antiperthite)+alkali feldspar (perthite~mesoperthite). Fine-grained orthopyroxene occurs around sapphirine. (b) A98021105A: Granular orthopyroxene and garnet grains are concentrated. Symplectite of sapphirine-orthopyroxene-plagioclase occurs around garnet. (c) A98021102H: Brownish green spinel constitutes the rock. Spinel and orthopyroxene are generally surrounded by sapphirine and garnet, respectively. (d) A98021003E: Idiomorphic sapphirine grains are developed in the matrix of orthopyroxene, garnet, plagioclase and alkali feldspar.

sapphirine and plagioclase (Figs. 3b and 4b). Garnet and orthopyroxene show granular texture. Sapphirine-orthopyroxene-plagioclase symplectite is formed around garnet. Sillimanite and cordierite are also present locally. Sillimanite is generally idiomorphic.

A98021102H: Spinel-bearing portion. Major constituent minerals are spinel, sapphirine, orthopyroxene, garnet, plagioclase and alkali feldspar. Sapphirine and garnet surround spinel and orthopyroxene, respectively (Fig. 4c). Corundum is locally accompanied by spinel. Retrograde biotite commonly occurs.

A98021003E: Idiomorphic sapphirine-rich portion (Figs. 3d and 4d). Constituent minerals are sapphirine, orthopyroxene, garnet, plagioclase and alkali feldspar (perthite-mesoperthite). Exsolution lamellae of rutile are observed in sapphirine. Garnet locally occurs between sapphirine and orthopyroxene (Fig. 15a).

Rutile is common in every rock type described above. Zircon and monazite are also minor.

2.2. Corundum-spinel-sapphirine-phlogopite gneiss (A98013107)

This occurs as a block (*ca.* 2 m in diameter) in the alternation of orthopyroxene-bearing quartzo-feldspathic gneiss and mafic granulite (Fig. 5a). Idiomorphic and

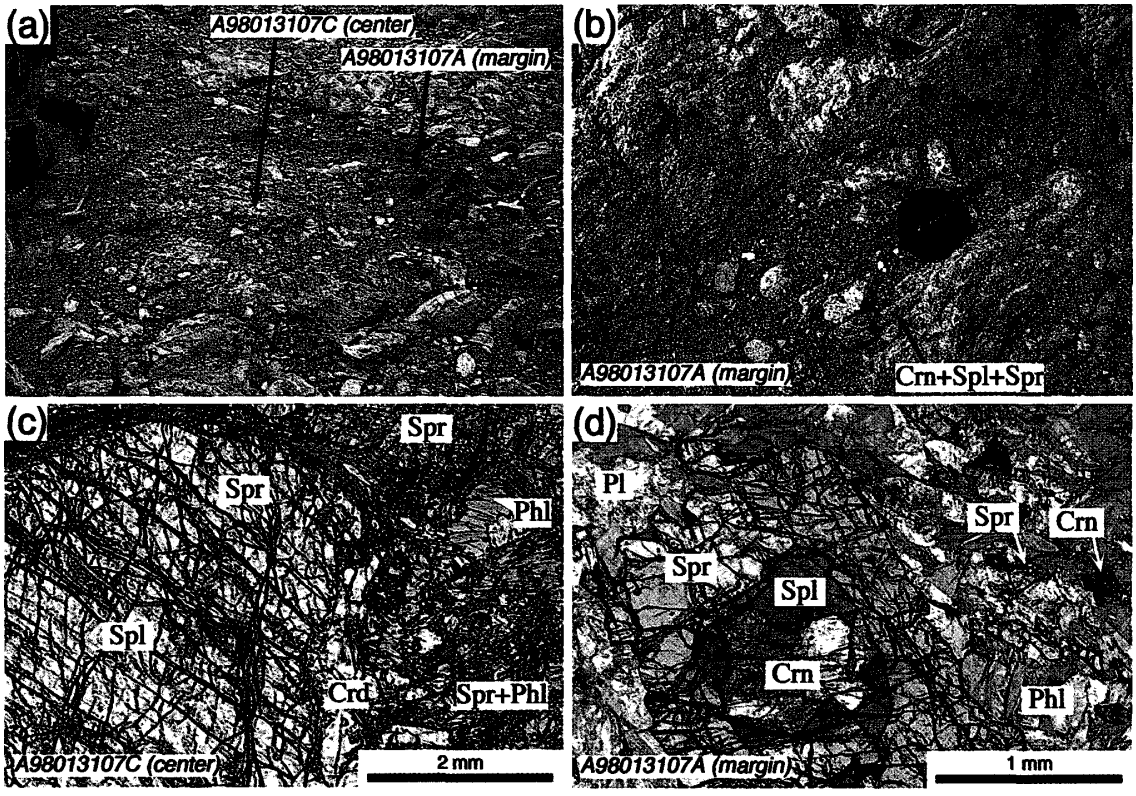

Fig. 5. Corundum-spinel-sapphirine-phlogopite-bearing gneiss from Unit II. (a) Field occurrence of the block of corundum-spinel-sapphirine-phlogopite gneiss. (b) Close up view of the marginal portion of the block. Idiomorphic and porphyroblastic pseudomorph after corundum, which is mostly replaced by spinel and sapphirine, is present in the phlogopite-rich matrix. (c) Photomicrograph of the sample A98013107C. Spinel (X_{Mg}=0.80–0.84) and sapphirine (X_{Mg}=0.93–0.94) have extremely magnesian compositions and are colorless in the thin section. Plane-polarized light. (d) Photomicrograph of sample A98013107A. Green spinel (X_{Mg}=0.46–0.49) and pale blue sapphirine (X_{Mg}=0.81–0.84) constitute the rock. Plane-polarized light.

porphyroblastic pseudomorph after corundum, which is mostly replaced by spinel and sapphirine, is present in phlogopite-rich matrix (Fig. 5b). Spinel encloses corundum, and both of them are surrounded by sapphirine. Phlogopite, plagioclase, sapphirine, corundum and subordinate cordierite constitute the matrix of the rock. Phlogopite, spinel and sapphirine in the central part of the block (A98013107C, Fig. 5c) are of paler color than those in the marginal part (A98013107A, Fig. 5d), and reflect compositional variation of Mg/(Mg+Fe), the ratio increasing toward the center (Tables 1 and 2).

2.3. Spinel-sapphirine-garnet-orthopyroxene gneiss (A98012902)

This is enclosed within leucocratic quartzo-feldspathic gneiss (Figs. 6a and b). Garnet and orthopyroxene are distributed separately from each other and form monomineralic aggregates respectively. Plagioclase monomineralic thin veins (<5 mm) are distributed between the garnet and orthopyroxene aggregates (Figs. 6b and c). Spinel, sapphirine and sillimanite are associated with garnet and are commonly included in garnet (Fig. 6d). Corundum is sometimes accompanied by spinel. Rutile is common in the rock. A98012902D and A98012902J are the garnet and orthopyroxene rich portions

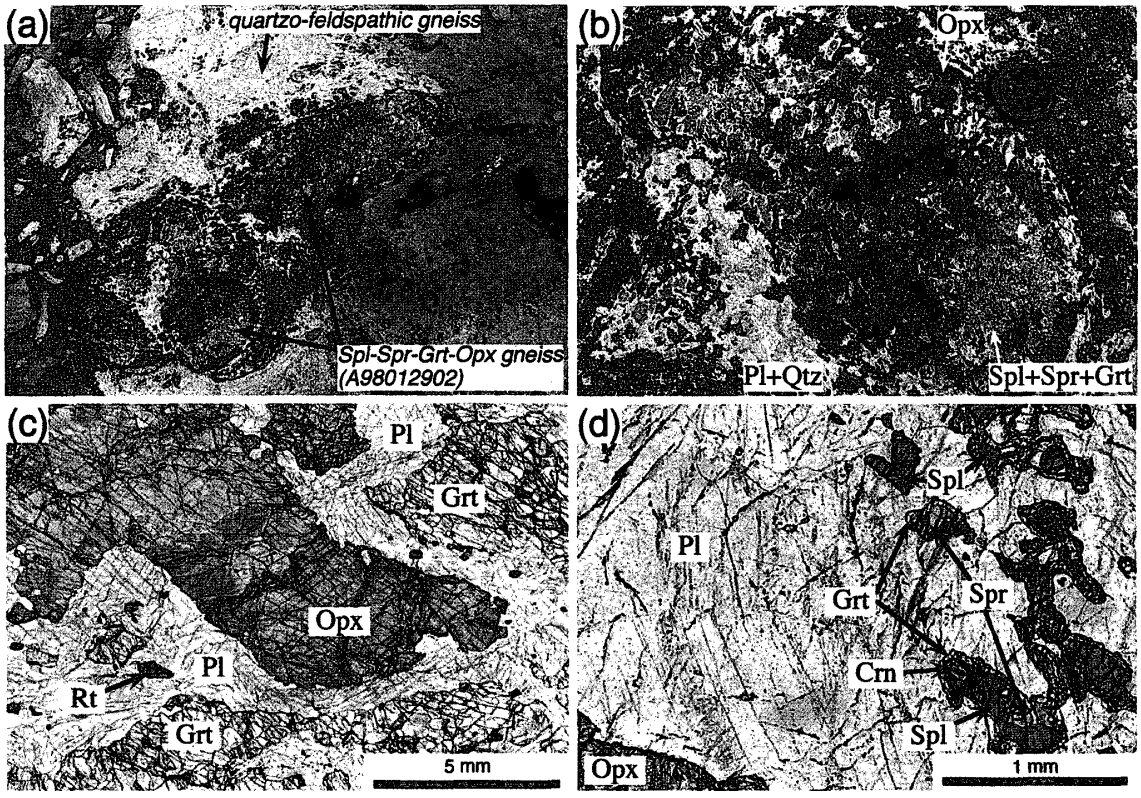

Fig. 6. Spinel-sapphirine-garnet-orthopyroxene gneiss from Unit II. (a) Field occurrence of the spinel-sapphirine-garnet-orthopyroxene gneiss surrounded by leucocratic quartzo-feldspathic gneiss (A98012902). (b) Close up view of the gneiss. Plagioclase monomineralic thin veins are distributed between the garnet and the orthopyroxene aggregates and are also connected to the relatively voluminous quartzo-feldspathic vein. (c) Photomicrograph of sample A98012902P. Plagioclase monomineralic thin veins are distributed between the garnet and the orthopyroxene aggregates. Plane-polarized light. (d) Photomicrograph of sample A98012902I. Spinel, sapphirine and corundum are commonly surrounded by garnet. Plane-polarized light.

in the aluminous block. A98012902I is the spinel- and corundum-bearing portion. A98012902P is the marginal portion of the block and is adjacent to the surrounding quartzo-feldspathic gneiss.

2.4. Spinel-corundum-sapphirine-garnet-orthopyroxene gneiss (A98012805B)

This occurs as a pod in felsic gneiss. Garnet and orthopyroxene are distributed separately from each other and form monomineralic aggregates. Plagioclase (or alkali feldspar) thin veins are present between garnet and orthopyroxene aggregates. Sapphirine, spinel and corundum are generally accompanied by or sometimes included in garnet and plagioclase. Quartz is rarely present and is restricted to alkali feldspar veins. Rutile is common.

3. Mineral Chemistry

Chemical analyses of constituent minerals were performed using an electron microprobe with an wavelength-dispersive X-ray analytical system (JEOL JXA-8800M) at the National Institute of Polar Research. Oxide ZAF correction was applied to the analyses. Probe current was kept at about 8 nA with accelerating voltage at 15 kV. Synthesized pure oxides and natural minerals were used for standards. Chemical features and representative analyses of constituent minerals in the aluminous gneisses are summarized in Tables 1 and 2.

3.1. Sapphirine

The Mg/(Mg+Fe) ratio ($=X_{Mg}$) of sapphirine generally ranges from 0.76 to 0.85, but up to 0.94 at the central portion of the corundum-phlogopite block (A98013107C). It has pleochroism of colorless to pale blue. But the high-Mg grains (X_{Mg} >0.9) are colorless. Sapphirine commonly shows weak compositional zoning, with Al-increasing and Si-decreasing toward the rim (Fig. 7). In sample A98013107, the sapphirine porphyroblast enclosing corundum and spinel has higher Al content up to 9.3 cations per 20 oxygen formula units than that in the matrix. In sample A98021106A, up to 2.2 wt% Cr_2O_3 is contained in sapphirine. Porphyroblastic sapphirine in sample A98021106A has exsolution lamellae of quartz.

3.2. Orthopyroxene

X_{Mg} of orthopyroxene ranges from 0.7 to 0.8. Orthopyroxene contains more than 10 wt% Al_2O_3 in the core, decreasing toward the rim (Fig. 8). Garnet and sapphirine occur in the grain boundary of orthopyroxene as exsolution products from high-Al orthopyroxene.

3.3. Garnet

Garnet in the aluminous gneisses is characterized by high pyrope content up to 60 mol% and low grossular (<4 mol%) and spessartine (<1 mol%) contents. Coarse grains have compositional zoning of Fe and Ca increasing and Mg decreasing toward the rim (Fig. 9), reflecting retrograde intracrystalline element diffusion. Fine grains and exsolution products in the grain boundary of orthopyroxene have lower X_{Mg} than in the core of the coarse grains.

Table 2. Representative microprobe analyses of constituent minerals.

mineral	Sapphirine										Orthopyroxene									
	Unit I : A9802-				Unit II : A9801-						Unit I : A9802-				Unit II : A9801-					
sample	1106A	1105A	1102H	1003E	3107A	3107C	2902D	2902I	2902J	2805B	1106A	1105A	1102H	1003E	2902D	2902I	2902J	2902P	2805B	
point	59	12	141	1	28	55	58	9	2	68	65	5	152	116	24	56	28	43	42	
wt %																				
SiO_2	14.89	13.65	14.43	14.14	12.89	14.29	14.93	14.06	13.90	13.99	51.56	51.40	50.91	52.19	49.69	49.25	48.42	49.39	50.06	
TiO_2	0.00	0.08	0.04	0.02	0.02	0.04	0.10	0.06	0.04	0.03	0.12	0.34	0.10	0.13	0.12	0.14	0.12	0.20	0.14	
Al_2O_3	58.57	62.60	60.23	61.15	64.23	64.10	59.55	61.39	62.33	60.97	7.65	8.14	8.64	8.49	10.55	9.12	10.33	9.23	9.46	
Cr_2O_3	1.83	0.05	0.72	0.53	0.00	0.00	0.00	0.02	0.05	0.06	0.26	0.03	0.17	0.07	0.00	0.01	0.00	0.05	0.00	
FeO*	7.12	5.60	7.25	7.19	6.14	2.61	8.73	8.24	7.27	7.97	14.56	14.09	14.89	13.67	15.44	18.78	17.43	18.39	17.29	
MnO	0.04	0.06	0.16	0.08	0.04	0.04	0.05	0.07	0.00	0.05	0.07	0.05	0.08	0.11	0.05	0.20	0.12	0.08	0.14	
ZnO	0.02	0.03	0.00	0.00	0.00	0.09	0.01	0.09	0.00	0.00	0.00	0.00	0.05	0.01	0.08	0.01	0.07	0.11	0.02	
MgO	17.03	17.37	16.72	16.90	16.86	19.61	16.47	15.61	17.24	17.24	26.31	26.60	25.38	26.76	24.00	22.52	23.63	22.87	22.88	
CaO	0.02	0.00	0.00	0.01	0.02	0.08	0.00	0.00	0.01	0.00	0.03	0.05	0.08	0.10	0.00	0.01	0.04	0.09	0.09	
Na_2O	0.04	0.00	0.04	0.00	0.00	0.01	0.03	0.01	0.01	0.05	0.03	0.22	0.00	0.05	0.00	0.00	0.03	0.00	0.04	
K_2O	0.00	0.00	0.00	0.00	0.00	0.00	0.00	0.00	0.00	0.00	0.00	0.00	0.00	0.00	0.00	0.00	0.00	0.00	0.00	
total	99.56	99.44	99.59	100.02	100.20	100.87	99.87	99.55	100.85	100.36	100.59	100.92	100.30	101.58	99.93	100.04	100.19	100.41	100.12	
cations	O = 20										O = 6									
Si	1.784	1.617	1.723	1.680	1.519	1.647	1.784	1.683	1.635	1.662	1.835	1.820	1.818	1.829	1.784	1.798	1.757	1.794	1.811	
Ti	0.000	0.007	0.004	0.002	0.002	0.003	0.009	0.005	0.004	0.003	0.003	0.009	0.003	0.003	0.003	0.004	0.003	0.005	0.004	
Al	8.270	8.742	8.478	8.561	8.922	8.705	8.388	8.659	8.641	8.537	0.321	0.340	0.364	0.351	0.446	0.392	0.442	0.395	0.403	
Cr	0.173	0.005	0.068	0.050	0.000	0.000	0.000	0.002	0.005	0.006	0.007	0.001	0.005	0.002	0.000	0.000	0.000	0.001	0.000	
Fe	0.713	0.555	0.724	0.714	0.605	0.251	0.872	0.825	0.715	0.792	0.433	0.417	0.445	0.401	0.463	0.573	0.529	0.558	0.523	
Mn	0.004	0.006	0.016	0.008	0.004	0.004	0.005	0.007	0.000	0.005	0.002	0.001	0.002	0.003	0.002	0.006	0.004	0.002	0.004	
Zn	0.002	0.003	0.000	0.000	0.000	0.008	0.001	0.008	0.000	0.000	0.000	0.000	0.001	0.000	0.002	0.000	0.002	0.003	0.001	
Mg	3.042	3.069	2.977	2.992	2.963	3.368	2.935	2.785	3.023	3.054	1.396	1.404	1.351	1.398	1.284	1.226	1.278	1.238	1.234	
Ca	0.003	0.000	0.000	0.001	0.003	0.010	0.000	0.000	0.001	0.000	0.001	0.002	0.003	0.004	0.000	0.000	0.002	0.003	0.003	
Na	0.008	0.000	0.009	0.000	0.000	0.002	0.007	0.002	0.002	0.012	0.002	0.015	0.000	0.003	0.000	0.000	0.002	0.000	0.003	
K	0.000	0.000	0.000	0.000	0.000	0.000	0.000	0.000	0.000	0.000	0.000	0.000	0.000	0.000	0.000	0.000	0.000	0.000	0.000	
total	13.999	14.004	13.999	14.008	14.018	13.998	14.001	13.976	14.026	14.071	4.000	4.009	3.992	3.994	3.984	3.999	4.019	3.999	3.986	
X_{Mg}	0.81	0.85	0.80	0.81	0.83	0.93	0.77	0.77	0.81	0.79	0.76	0.77	0.75	0.78	0.73	0.68	0.71	0.69	0.70	

* total Fe as FeO

Table 2 (Continued).

mineral	Garnet									Spinel						Phlogopite	
	Unit I : A9802-				Unit II : A9801-					A9802-	Unit II : A9801-					Unit II : A9801-	
sample	1106A	1105A	1102H	1003E	2902D	2902I	2902J	2902P	2805B	1102H	3107A	3107C	2902I	2902P	2805B	3107A	3107C
point	86	49	143	73	37	67	18	20	51	132	7	51	5	22	160	2-6	2-19
wt %																	
SiO_2	40.97	41.37	40.07	40.82	40.54	40.66	41.48	41.05	40.34	0.03	0.01	0.01	0.00	0.07	0.00	40.93	42.71
TiO_2	0.03	0.02	0.00	0.04	0.01	0.02	0.00	0.10	0.00	0.00	0.00	0.06	0.00	0.23	0.00	1.92	1.13
Al_2O_3	23.13	23.39	22.33	23.51	23.25	23.29	23.47	23.39	22.91	63.42	64.55	68.58	64.60	66.98	62.69	13.92	13.62
Cr_2O_3	0.11	0.00	0.06	0.00	0.00	0.00	0.00	0.00	0.00	2.37	0.00	0.00	0.03	0.07	0.00	0.00	0.01
FeO*	21.63	18.29	23.10	17.49	22.13	21.94	20.69	21.64	23.04	20.08	22.41	9.81	20.39	15.79	13.75	4.38	1.47
MnO	0.11	0.37	0.44	0.53	0.15	0.31	0.42	0.42	0.40	0.09	0.36	0.04	0.02	0.00	0.00	0.04	0.00
ZnO	0.01	0.02	0.05	0.00	0.00	0.04	0.07	0.00	0.00	0.16	0.89	0.16	1.01	1.05	15.52	0.00	0.00
MgO	14.46	16.42	13.67	16.38	14.02	13.99	14.94	13.33	13.00	14.08	11.93	21.60	13.80	16.30	9.15	24.25	26.90
CaO	0.92	1.00	1.33	1.51	0.40	0.51	0.50	0.40	0.91	0.02	0.01	0.02	0.00	0.01	0.02	0.00	0.01
Na_2O	0.00	0.04	0.00	0.00	0.00	0.04	0.01	0.02	0.01							0.30	0.98
K_2O	0.00	0.00	0.00	0.00	0.00	0.00	0.00	0.00	0.00	0.00	0.00	0.00	0.00	0.00	0.00	10.65	9.39
F																5.26	5.04
-O																-2.21	-2.12
total	101.37	100.92	101.05	100.28	100.50	100.80	101.58	100.35	100.61	100.25	100.16	100.28	99.85	100.50	101.13	99.44	99.14
cations	O = 12									O = 4						O = 22	
Si	3.003	3.003	2.983	2.980	2.993	2.998	3.013	3.030	3.004	0.001	0.000	0.000	0.000	0.002	0.000	5.759	5.890
Ti	0.002	0.001	0.000	0.002	0.001	0.001	0.000	0.006	0.000	0.000	0.000	0.001	0.000	0.004	0.000	0.203	0.117
Al	1.998	2.001	1.959	2.022	2.023	2.024	2.009	2.034	2.011	1.954	2.005	1.996	1.995	2.008	2.004	2.308	2.214
Cr	0.006	0.000	0.004	0.000	0.000	0.000	0.000	0.000	0.000	0.049	0.000	0.000	0.001	0.001	0.000	0.000	0.001
Fe	1.326	1.110	1.438	1.068	1.366	1.353	1.256	1.336	1.435	0.439	0.494	0.203	0.447	0.336	0.312	0.515	0.170
Mn	0.007	0.022	0.028	0.033	0.009	0.019	0.026	0.026	0.025	0.002	0.008	0.001	0.000	0.000	0.000	0.005	0.000
Zn	0.001	0.001	0.003	0.000	0.000	0.002	0.003	0.000	0.000	0.003	0.017	0.003	0.019	0.020	0.311	0.000	0.000
Mg	1.580	1.777	1.517	1.783	1.543	1.538	1.618	1.467	1.443	0.549	0.469	0.795	0.539	0.618	0.370	5.086	5.531
Ca	0.072	0.078	0.106	0.118	0.032	0.040	0.039	0.032	0.073	0.001	0.000	0.001	0.000	0.000	0.001	0.000	0.001
Na	0.000	0.006	0.000	0.000	0.000	0.006	0.001	0.003	0.001							0.082	0.262
K	0.000	0.000	0.000	0.000	0.000	0.000	0.000	0.000	0.000	0.000	0.000	0.000	0.000	0.000	0.000	1.912	1.652
total	7.995	7.999	8.038	8.006	7.967	7.981	7.965	7.934	7.992	2.998	2.993	3.000	3.001	2.989	2.998	15.870	15.838
X_{Mg}	0.54	0.62	0.51	0.63	0.53	0.53	0.56	0.52	0.50	0.56	0.49	0.80	0.55	0.65	0.54	0.91	0.97
alm	0.45	0.37	0.47	0.36	0.46	0.46	0.43	0.47	0.48	-	-	-	-	-	-	-	-
prp	0.53	0.59	0.49	0.59	0.52	0.52	0.55	0.51	0.49	-	-	-	-	-	-	-	-
grs	0.02	0.03	0.03	0.04	0.01	0.01	0.01	0.01	0.02	-	-	-	-	-	-	-	-
sps	0.00	0.01	0.01	0.01	0.00	0.01	0.01	0.01	0.01	-	-	-	-	-	-	-	-

* total Fe as FeO

Table 2 (Continued).

mineral	Plagioclase											Alkali feldspar			
	Unit I : A9802-					Unit II : A9801-						Unit I : A9802-			A9801-
sample	1106A	1105A	1102H	1102H	1003E	3107A	2902D	2902I	2902J	2902P	2805B	1106A	1102H	1003E	2805B
point	80	16	98	104	5	16	59	92	10	13	186	83	105	7	170
wt %			core	rim											
SiO_2	61.79	60.21	50.37	57.14	57.31	62.71	64.66	64.98	63.20	64.79	62.88	65.23	65.07	64.54	63.06
TiO_2	0.00	0.06	0.00	0.00	0.00	0.04	0.02	0.00	0.07	0.00	0.00	0.00	0.00	0.00	0.00
Al_2O_3	24.60	24.67	31.81	27.08	27.10	23.43	21.81	21.89	22.07	22.14	23.32	18.73	18.47	18.68	18.63
Cr_2O_3	0.03	0.00	0.00	0.01	0.00	0.03	0.00	0.04	0.03	0.09	0.00	0.06	0.01	0.00	0.01
FeO*	0.00	0.04	0.00	0.02	0.05	0.15	0.00	0.04	0.32	0.01	0.10	0.00	0.00	0.00	0.00
MnO	0.00	0.02	0.03	0.12	0.05	0.00	0.00	0.09	0.03	0.02	0.03	0.00	0.03	0.00	0.00
MgO	0.00	0.03	0.01	0.00	0.03	0.00	0.00	0.00	0.00	0.00	0.00	0.00	0.00	0.00	0.00
CaO	5.83	6.43	14.46	9.00	8.75	4.46	2.70	2.86	3.36	3.09	4.23	0.20	0.24	0.18	0.03
Na_2O	8.28	7.90	3.13	6.23	6.38	8.73	9.81	9.71	9.65	9.58	9.01	1.54	1.45	1.62	1.10
K_2O	0.14	0.19	0.08	0.35	0.10	0.06	0.39	0.48	0.33	0.56	0.20	14.58	14.44	14.48	14.07
BaO	0.00	0.00	0.16	0.01	0.00	0.05	0.07	0.25	0.15	0.02	0.14	0.12	0.27	0.47	2.74
total	100.67	99.55	100.05	99.96	99.77	99.66	99.46	100.34	99.21	100.30	99.91	100.46	99.98	99.97	99.64
cations	O = 8											O = 8			
Si	2.724	2.693	2.294	2.566	2.572	2.778	2.857	2.861	2.820	2.849	2.786	2.987	2.995	2.980	2.964
Ti	0.000	0.002	0.000	0.000	0.000	0.001	0.001	0.000	0.002	0.000	0.000	0.000	0.000	0.000	0.000
Al	1.278	1.300	1.708	1.433	1.433	1.223	1.136	1.136	1.161	1.147	1.218	1.011	1.002	1.016	1.032
Cr	0.001	0.000	0.000	0.000	0.000	0.001	0.000	0.001	0.001	0.003	0.000	0.002	0.000	0.000	0.000
Fe	0.000	0.001	0.000	0.001	0.002	0.006	0.000	0.001	0.012	0.000	0.004	0.000	0.000	0.000	0.000
Mn	0.000	0.001	0.001	0.005	0.002	0.000	0.000	0.003	0.001	0.001	0.001	0.000	0.001	0.000	0.000
Mg	0.000	0.002	0.001	0.000	0.002	0.000	0.000	0.000	0.000	0.000	0.000	0.000	0.000	0.000	0.000
Ca	0.275	0.308	0.705	0.433	0.420	0.212	0.128	0.135	0.161	0.146	0.201	0.010	0.012	0.009	0.002
Na	0.708	0.685	0.276	0.542	0.555	0.750	0.840	0.829	0.835	0.817	0.774	0.137	0.129	0.145	0.100
K	0.008	0.011	0.005	0.020	0.006	0.003	0.022	0.027	0.019	0.031	0.011	0.852	0.848	0.853	0.844
Ba	0.000	0.000	0.003	0.000	0.000	0.001	0.001	0.004	0.003	0.000	0.002	0.002	0.005	0.009	0.050
total	4.994	5.003	4.993	5.000	4.992	4.975	4.985	4.997	5.015	4.994	4.997	5.001	4.992	5.012	4.992
an	0.28	0.31	0.71	0.44	0.43	0.22	0.13	0.14	0.16	0.15	0.20	0.01	0.01	0.01	0.00
ab	0.71	0.68	0.28	0.54	0.56	0.78	0.85	0.84	0.82	0.82	0.79	0.14	0.13	0.14	0.11
or	0.01	0.01	0.01	0.02	0.01	0.00	0.02	0.03	0.02	0.03	0.01	0.85	0.86	0.85	0.89

* total Fe as FeO

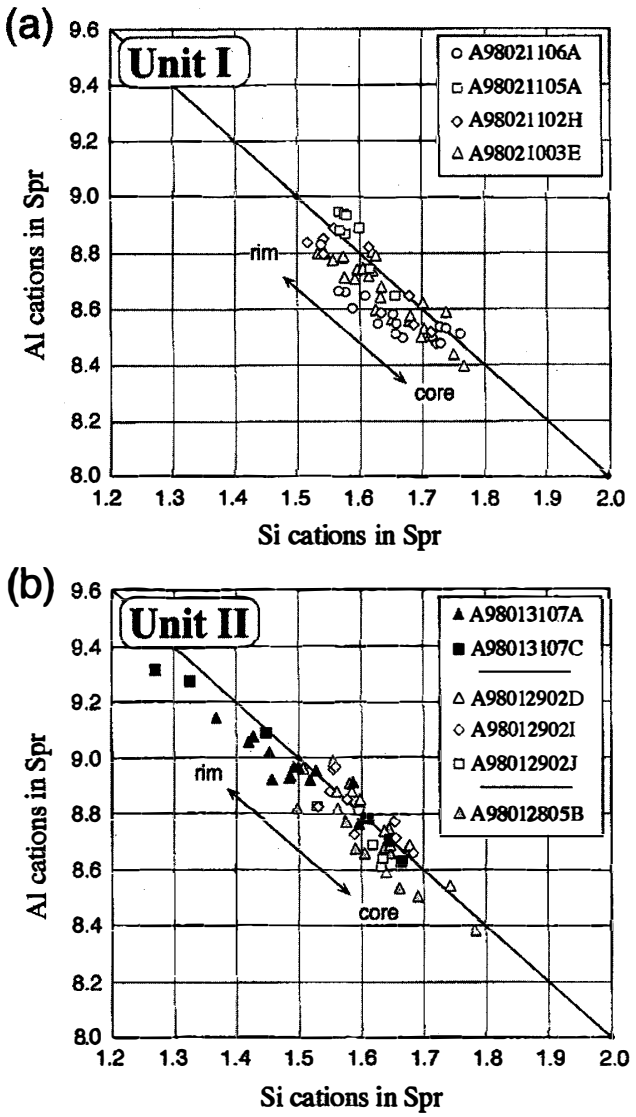

Fig. 7. Sapphirine compositions in terms of Al cations and Si cations per 20-oxygen formula unit. The compositional trend parallels the Tschermak substitution. Si content in sapphirine monotonously decreases (Al increasing) toward the rim. (a) Sapphirine in the aluminous gneiss from Unit I. (b) Sapphirine in the aluminous gneiss from Unit II.

3.4. Spinel

X_{Mg} of spinel generally ranges from 0.46 to 0.65, except that from the central portion of the corundum-phlogopite block (A98013107C), which ranges up to 0.81. Spinel in the sample A98012805B contains ZnO of up to 16 wt%.

3.5. Phlogopite

Non-retrograde phlogopite is contained only in the sample A98013107. X_{Mg} ranges from 0.90 to 0.97. Phlogopite in A98013107C, which is collected from the center portion of the corundum-phlogopite block, has higher X_{Mg} than that in A98013107A, which is from the marginal portion of the block. Both of them contain about 5 wt% of F.

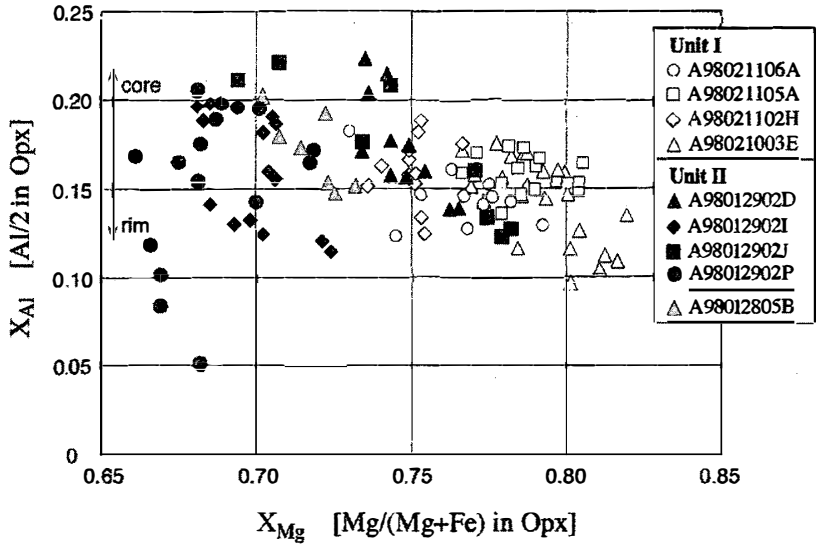

Fig. 8. Orthopyroxene X_{Mg}-X_{Al} relationships. X_{Al}=Al cations/2 per 6-oxygen formula unit. Al content in orthopyroxene decreases toward the rim.

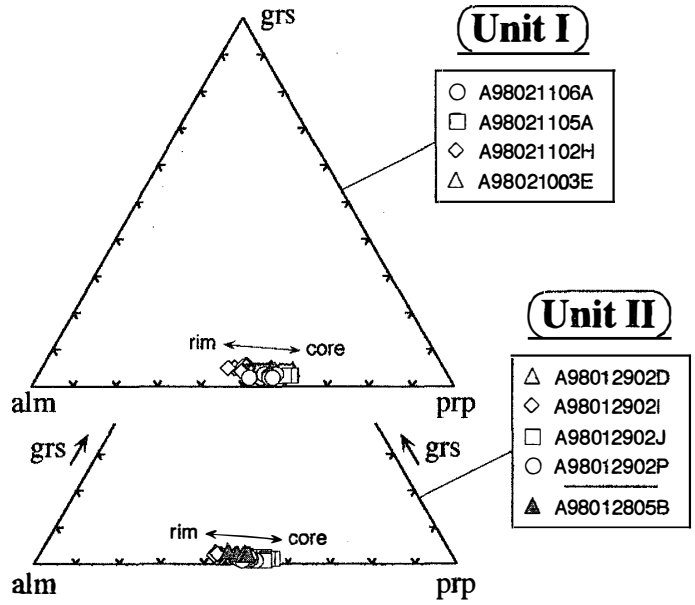

Fig. 9. Grossular (grs)-almandine (alm)-pyrope (prp) plot of garnet compositions in the aluminous gneisses. Pyrope content in garnet decreases with increasing almandine and grossular content toward the rim.

3.6. Plagioclase

Chemical compositions of plagioclase are shown in Fig. 10. Plagioclase in the aluminous gneisses around the ultramafic layer (A98021106A, A98021105A, A98021102H, A98021003E) is characterized by relatively high anorthite content. Plagioclase in A98021102H and A98021003E show compositional zoning of decreasing anorthite content toward the rim, from 75 mol% to 48 mol% and from 47 mol% to 37

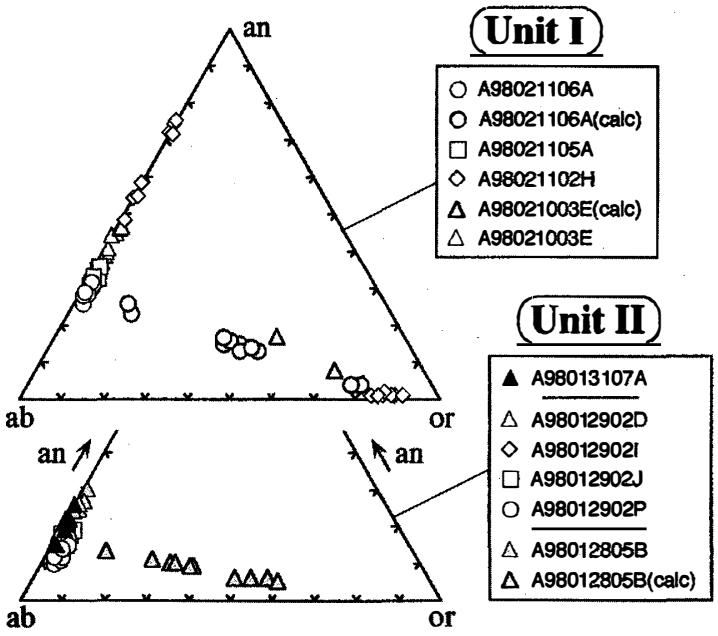

Fig. 10. Anorthite (an)-albite (ab)-orthoclase(or) plot of feldspar compositions in the aluminous gneisses. Heavy symbols (labeled 'calc') are calculated compositions from modal proportions of host and lamellae multiplied by chemical compositions of each.

mol%, respectively. Some plagioclase grains in the samples A98021106A and A98021003E have antiperthitic exsolution lamellae.

Plagioclase from the other aluminous gneisses has relatively lower anorthite content than the above. Plagioclase occurring as a thin vein between garnet and orthopyroxene in the sample A98012902 shows weak compositional zoning of increasing anorthite content (less than 2 mol percentage points) from the garnet-side to the orthopyroxene-side.

3.7. Alkali feldspar (mesoperthite)

Occurrence of alkali feldspar is restricted in the aluminous gneisses around ultramafic rocks (A98021003E, A98021102H, A98021106A) or in the leucocratic portion of the aluminous gneiss (A98012805B). Chemical compositions of the analyzed alkali feldspar are represented in Fig. 10. Exsolution lamellae commonly develop (Fig. 11), and original mineral compositions of mesoperthite (and antiperthitic plagioclase) are estimated from modal proportions of host and lamellae multiplied by chemical compositions of each. Chemical compositions of mesoperthitic alkali feldspars are characterized by high anorthite content of up to 17 mol% (an:ab:or=17:43:40, in A98021106A). Alkali feldspars in the sample A98012805B show chemical zoning of wide compositional range from perthite (an:ab:or=5:36:59) to antiperthite (an:ab:or=13:63:14) almost continuously.

4. Discussion

4.1. Lithological and petrological features of the aluminous gneisses

Figure 12 illustrates the mineral compositions and mineral parageneses of the alumi-

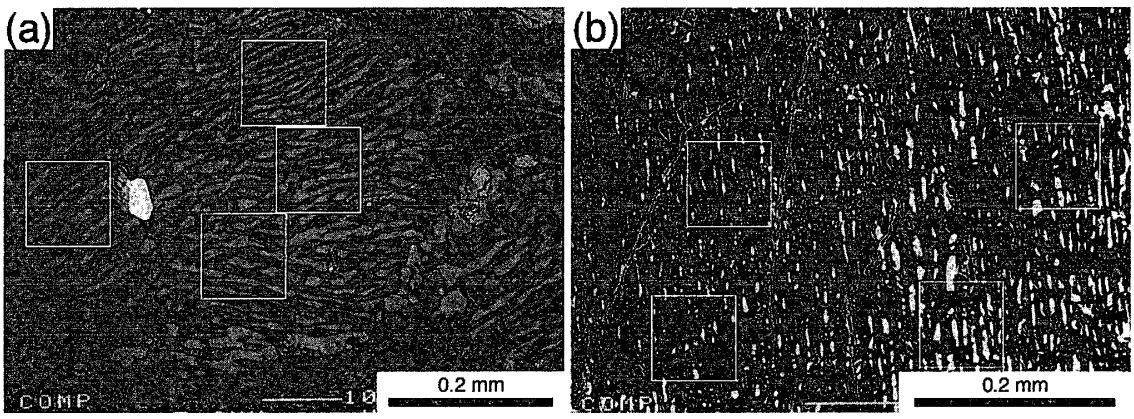

Fig. 11. Backscattered electron images of mesoperthitic feldspar in the aluminous gneisses. The bright portion represents K-feldspar composition and the dark portion is plagioclase composition. Squares indicate the area used for calculation of the volumetric proportions of host and lamellae formed by exsolution. (a) Mesoperthite from sample A98021106A. Plagioclase also occurs around the mesoperthite, and contains a small proportion of antiperthitic lamellae. (b) Mesoperthite~antiperthite from sample A98012805B. The volumetric proportion of lamellae (K-feldspar) increases from the orthopyroxene-side (left) to the garnet-side (right), and represents compositional zoning as shown in Fig. 10.

nous gneisses. The important feature is the quartz-free silica-undersaturated mineral parageneses composed of relatively high X_{Mg} phases. Sapphirine+garnet+orthopyroxene is the stable mineral paragenesis for all analyzed samples (A98021106A, A98021105A, A98021102H and A98021003E) from Unit I. Spinel is the additional constituent for A98021102H. Cordierite and sillimanite locally constitute the gneisses (A98021106A, A98021105A) and are considered to reflect differences of local bulk compositions. Some cordierite, sillimanite and garnet grains are obviously retrograde products, but it is difficult to judge whether the other cordierite, sillimanite and garnet grains are in the stable phase or not at the peak metamorphism from mineral textures and mineral compositions. A98012902 and A98012805B from Unit II also show similar mineral assemblages to those from Unit I, but sapphirine is commonly surrounded by garnet. This observation suggests that the sapphirine has possibly coexisted with garnet and orthopyroxene at the peak conditions, and that garnet is formed around sapphirine during retrograde metamorphism. A98012902 and A98012805B occasionally contain spinel, corundum and sillimanite, and are considered to reflect differences of local bulk compositions. Sapphirine+corundum+phlogopite is the stable mineral paragenesis for A98013107 in Unit II.

The occurrence of silica-undersaturated aluminous gneiss from Unit I (A98021106A, A98021105A, A98021102H and A98021003E) is restricted to layers between the ultramafic rock and quartzo-feldspathic rock. This suggests that the formation of the aluminous gneiss is originated from interaction (whether metasomatism or mixing accompanied by partial melting) between the ultramafic rock and the quartzo-feldspathic rock. However, the actual formation process is beyond the scope of this study.

A98012902 and A98012805B from Unit II are associated with leucocratic vein composed of quartz+feldspar (either plagioclase or plagioclase+alkali feldspar) or of monomineralic plagioclase. The leucocratic veins appear to have crystallized from melt,

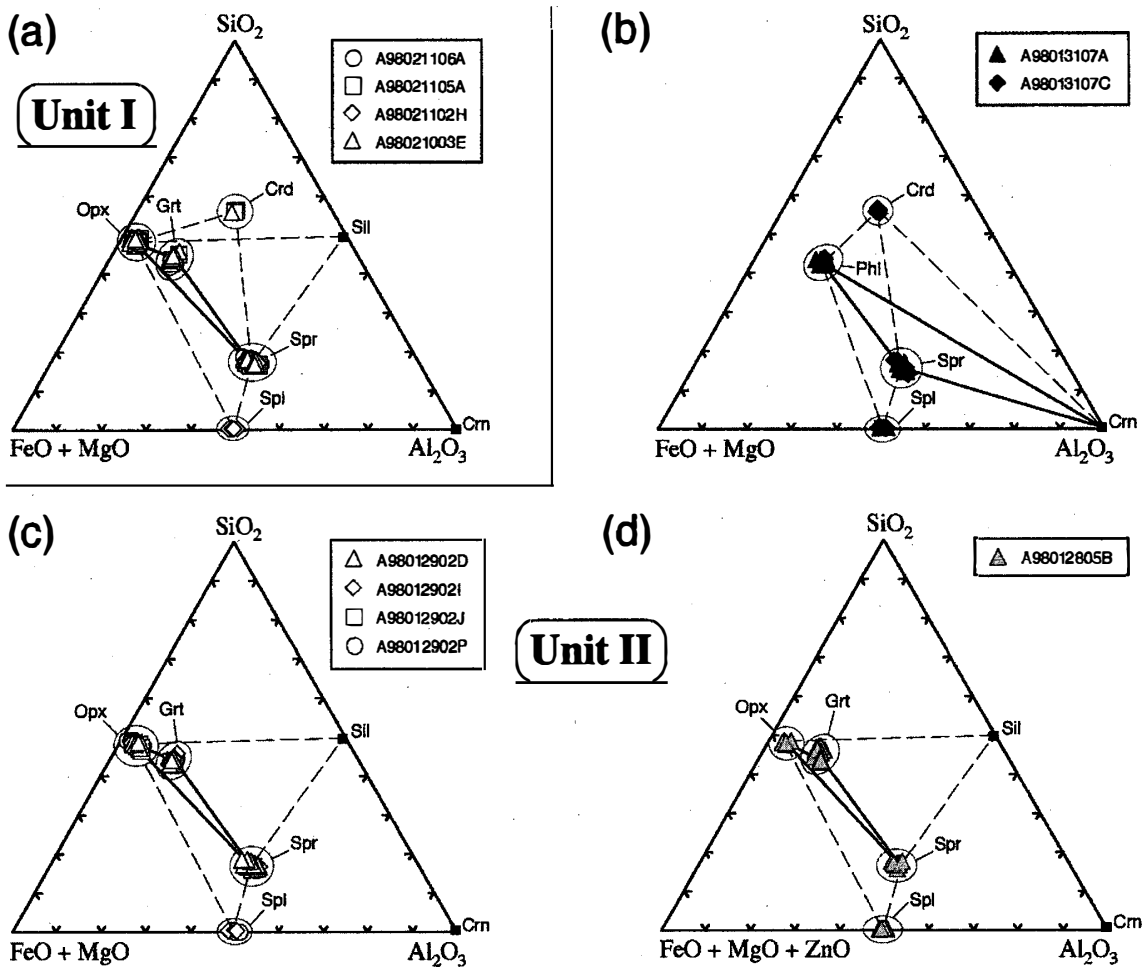

Fig. 12. SiO_2-Al_2O_3-(FeO+MgO) projection of the phases constituting the aluminous gneisses. Phlogopite is projected from K_2O. Solid lines represent initial mineral parageneses. Dashed lines indicate local or retrograde parageneses. (a) Aluminous gneisses from Unit I. (b) The sample A98013107 from Unit II. (c) The sample A98012902 from Unit II. (d) The sample A98012805B from Unit II. ZnO is added to FeO+MgO, because spinel in this sample contains up to 16 wt% of ZnO.

judging from the field occurrence (Figs. 6a and b), which suggests that the aluminous gneisses formed from partial melting.

A98013107 is composed of a large amount of F-bearing phlogopite with corundum-spinel-sapphirine porphyroblast. This represents not pelitic but rather ultramafic bulk chemical composition. Higher X_{Mg} of the constituent minerals in the center (A98013107C) of the block than those in the margin (A98013107A) indicates the compositional zonal structure of the block. It is difficult to judge whether this zonal structure of the block reflects original compositional variation or is formed through a process associated with metasomatism.

4.2. Metamorphic conditions of the aluminous gneisses

Quartz does not coexist with sapphirine, spinel or corundum in the aluminous gneisses discussed here. Metamorphic conditions cannot be constrained by the phase

relation because of the high degree of freedom in the system. Geothermobarometry using element partitioning between garnet and orthopyroxene (HARLEY, 1984a, b; corrected by FITZSIMONS and HARLEY, 1994) indicates equilibrium conditions of 800–1000°C and 0.5–1.0 GPa, from the garnet core having the highest pyrope content and the orthopyroxene core having the highest Al content (Figs. 13 and 14). The temperatures estimated here (800–1000°C) are lower than those estimated from mineral compositions of mesoperthitic alkali feldspar in the same sample indicating >1100°C (HOKADA *et al.*, 1999), and from the occurrence of sapphirine-quartz association in the central part of Tonagh Island suggesting >1030°C. Figure 14 illustrates the compositional zoning patterns of Mg and Ca in garnet and those of Fe and Al in orthopyroxene. Mg and Al components are enriched in cores of garnet and orthopyroxene, respectively, and these compositional zoning patterns are considered to reflect intracrystalline element diffusion during retrograde metamorphism. Al in orthopyroxene, which is modeled in the geobarometer (HARLEY, 1984a; corrected by FITZSIMONS and HARLEY, 1994), is less diffusive than Mg and Fe, which mainly contribute on the geothermometer (HARLEY, 1984b), and this implies that the temperature estimated from the geothermometer is underestimated compared to pressure from the geobarometer. Therefore, the pressure condition of 0.8–1.1 GPa is estimated for the thermal peak (1030–1100°C) using the geobarometer (solid and dashed lines in Fig. 13). *P-T* conditions of 600–700°C and 0.4–0.6 GPa (those from A98012902P representing the higher *P-T*, *ca.* 800°C and 0.8 GPa) are obtained

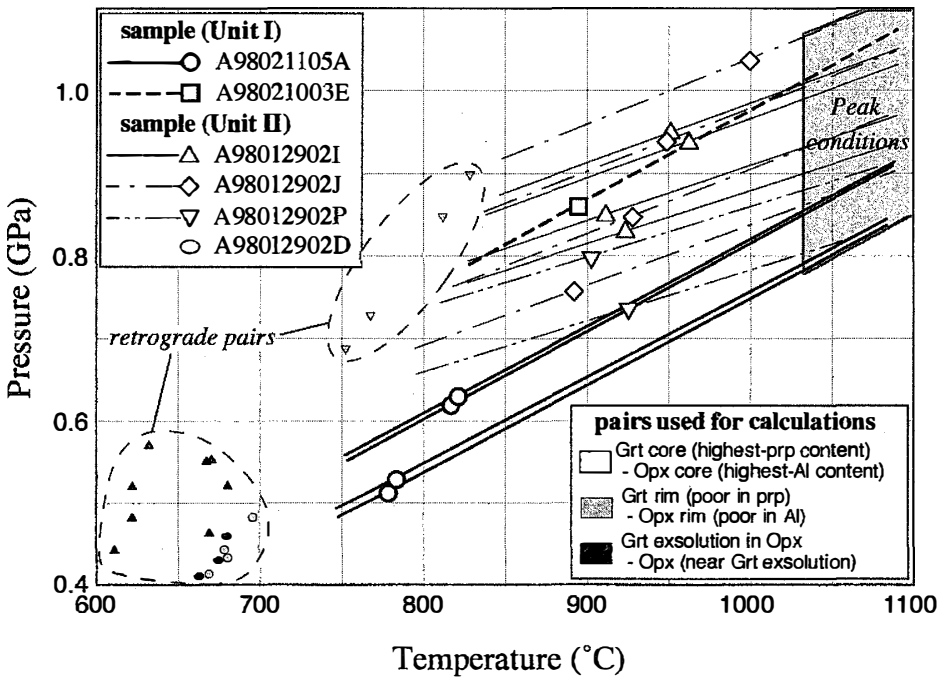

Fig. 13. P-T estimations for the aluminous gneisses from Tonagh Island using garnet-orthopyroxene geothermobarometers (HARLEY, 1984a,b; FITZSIMONS and HARLEY, 1994). Peak conditions are estimated from the geobarometry (solid and dashed lines, calculated using HARLEY, 1984a; corrected by FITZSIMONS and HARLEY, 1994) and temperatures obtained from other method. See text in detail.

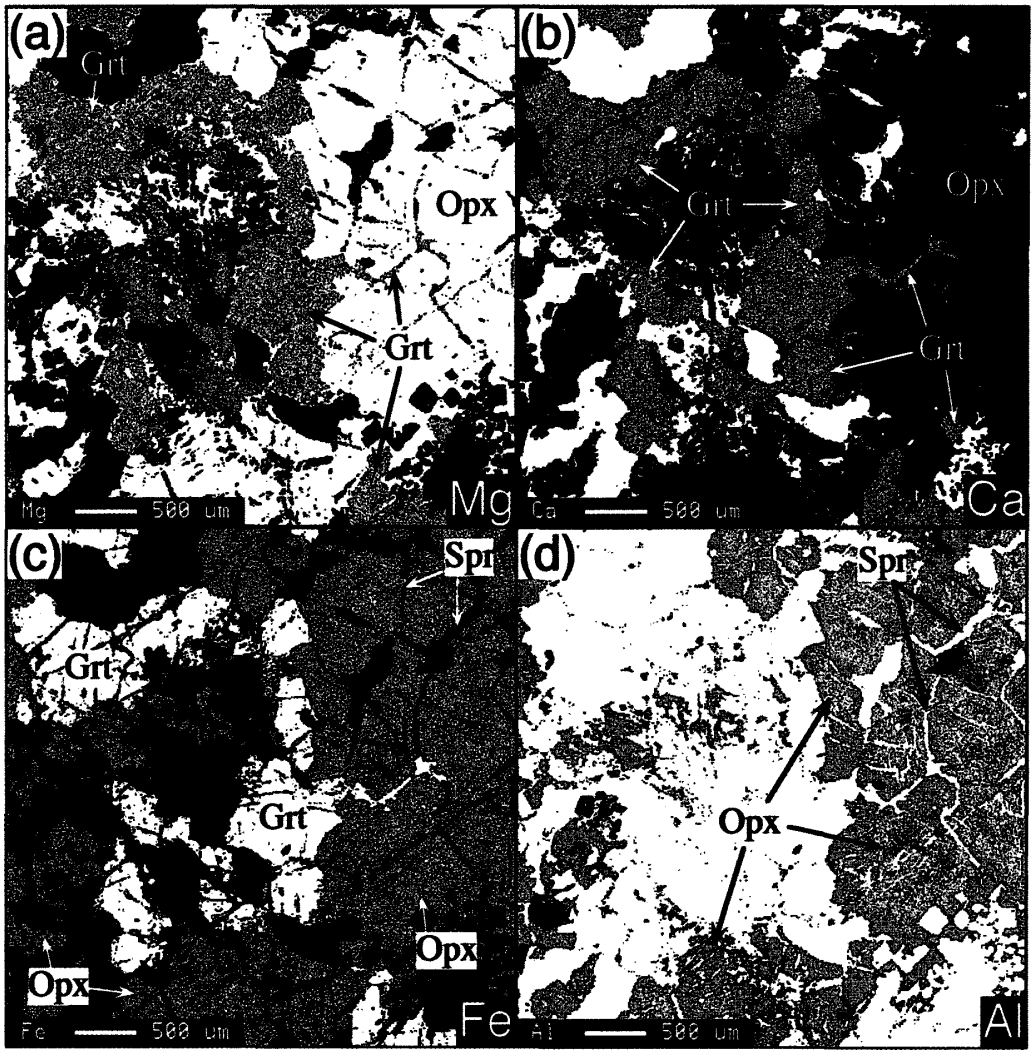

Fig. 14. X-ray concentration map of the sample A98021105A. A warm color represents higher-concentration (white is the highest) and a cold one is lower-concentration (black is the lowest), respectively. Garnet shows the compositional zoning of Mg-decreasing and Fe- and Ca-increasing toward the rim; and orthopyroxene shows compositional zoning of Al- and Fe-decreasing and Mg-increasing toward the rim. Exsolution of garnet and sapphirine occurs at the grain boundary of orthopyroxene. (a) X-ray map of Mg. (b) X-ray map of Ca. (c) X-ray map of Fe. (d) X-ray map of Al.

from element partitioning between the rims of garnet and orthopyroxene, and between the garnet exsolution and the adjacent portion of the host orthopyroxene. However, it is difficult to judge whether they are in equilibrium with each other or not, because retrograde reaction textures are commonly developed, as will be discussed below; not only intracrystalline diffusion but also retrograde reaction modify the chemical composition. In addition, a part of the garnet grain is considered to be crystallized from decomposition of orthopyroxene, suggesting a reaction relation.

A variety of reaction textures are observed around sapphirine and orthopyroxene, as follows (Fig. 15).

(1) Sapphirine+orthopyroxene → garnet

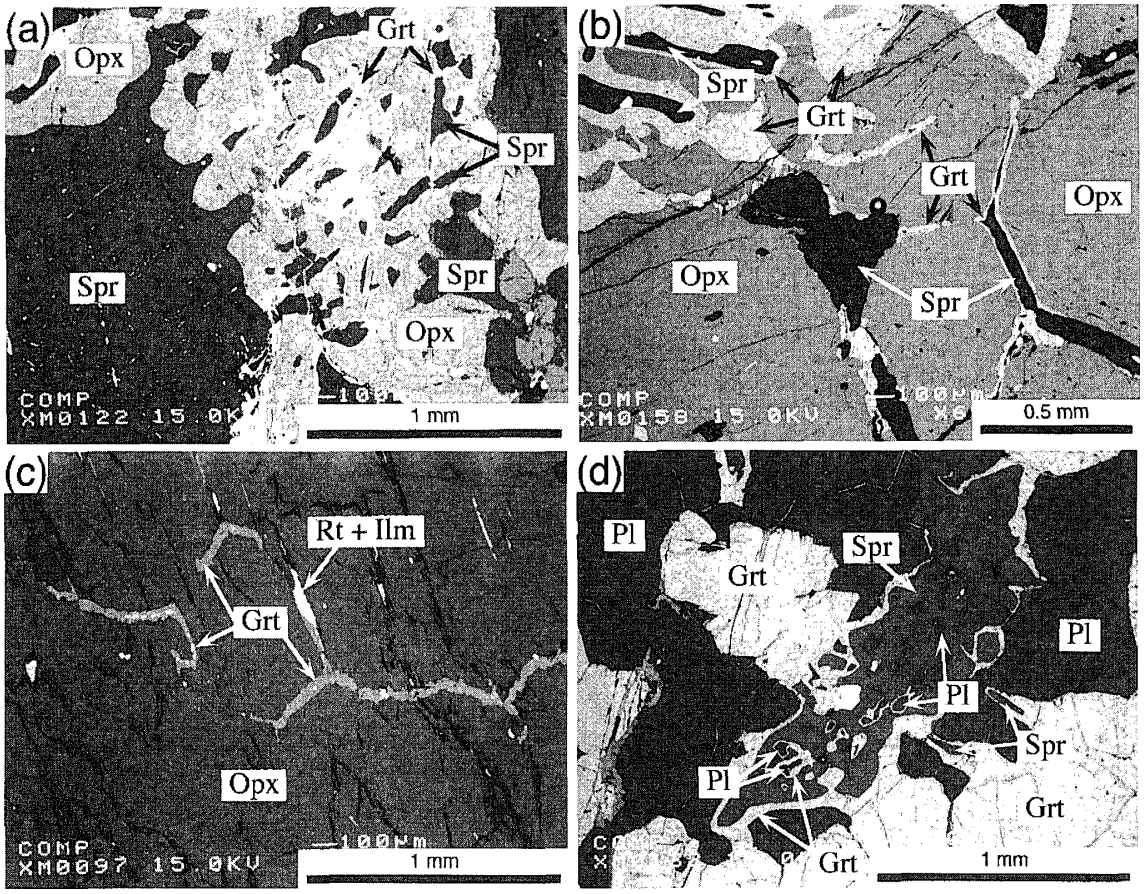

Fig. 15. Backscattered electron images of retrograde reaction textures in the aluminous gneisses. (a) Garnet is formed between sapphirine and orthopyroxene (A98021003E). (b) Exsolution of sapphirine after orthopyroxene; garnet is subsequently formed between sapphirine and orthopyroxene (A98012902D). (c) Exsolution of garnet after orthopyroxene (A98012902I). (d) Thin film of garnet surrounds sapphirine (A98012902J).

(2) Al-rich orthopyroxene → garnet+Al-poor orthopyroxene
(3) Al-rich orthopyroxene → sapphirine+Al-poor orthopyroxene
(4) Si-rich sapphirine → garnet+Si-poor sapphirine

The reaction (1) is observed as a texture of the garnet thin film occurring between sapphirine and orthopyroxene (Figs. 15a and b). It can be also expressed as the combination of reactions (2) and (4). Garnet and sapphirine exsolutions occur as thin films at the grain boundaries of orthopyroxene grains (Figs. 15b and c) and demonstrate reactions (2) and (3), respectively. Garnet surrounding sapphirine is observed commonly in the aluminous gneisses (Fig. 15d), and suggests that reaction (4) takes place. All of these reactions result from decreasing Al_2O_3 content in orthopyroxene or decreasing SiO_2 content in sapphirine during the retrograde stage (Figs. 7 and 8).

Acknowledgments

The authors express their sincere thanks to the members of JARE-39 and the crew of the icebreaker SHIRASE for their support during the 1997–1998 field season. T.H. is

also grateful to NIPR for enabling him to carry out the field work. Prof. K. SHIRAISHI, Dr. Y. MOTOYOSHI and Ms. S. SUZUKI are thanked for their discussion and encouragement. Some of the thin sections used in this study were prepared by Mr. S. OHNO. This manuscript was reviewed and improved by Dr. Y. MOTOYOSHI and two anonymous referees. Thanks are also due to them.

References

DALLWITZ, W.B. (1968): Coexisting sapphirine and quartz in granulites from Enderby Land, Antarctica. Nature, **219**, 476–477.

ELLIS, D.J., SHERATON, J.W., ENGLAND, R.N. and DALLWITZ, W.B. (1980): Osumilite-sapphirine-quartz granulites from Enderby Land Antarctica—mineral assemblages and reactions. Contrib. Mineral. Petrol., **72**, 123–143.

FITZSIMONS, I.C.W. and HARLEY, S.L. (1994): The influence of retrograde cation exchange on granulite *P-T* estimates and a convergence technique for the recovery of peak metamorphic conditions. J. Petrol., **35**, 543–576.

GREW, E.S. (1980): Sapphirine+quartz association from Archaean rocks in Enderby Land, Antarctica. Am. Mineral., **65**, 821–836.

GREW, E.S. (1982): Osumilite in the sapphirine-quartz terrane of Enderby Land, Antarctica: Implications for osumilite petrogenesis in the granulite facies. Am. Mineral., **67**, 762–787.

HARLEY, S.L. (1984a): The solubility of alumina in orthopyroxene coexisting with garnet in FeO-MgO-Al_2O_3-SiO_2 and CaO-FeO-MgO-Al_2O_3-SiO_2. J. Petrol., **25**, 665–696.

HARLEY, S.L. (1984b): An experimental study of the partitioning of Fe and Mg between garnet and orthopyroxene. Contrib. Mineral. Petrol., **86**, 359–373.

HARLEY, S.L. (1985): Garnet-orthopyroxene bearing granulites from Enderby Land, Antarctica: Metamorphic pressure-temperature-time evolution of the Archaean Napier Complex. J. Petrol., **26**, 819–856.

HARLEY, S.L. (1986): A sapphirine-cordierite-garnet-sillimanite granulite from Enderby Land, Antarctica: Implications for FMAS petrogenetic grids in the granulite facies. Contrib. Mineral. Petrol., **94**, 452–460.

HARLEY, S.L. (1987): A pyroxene-bearing metaironstone and other pyroxene-granulites from Tonagh Island, Enderby Land, Antarctica: Further evidence for very high temperature (>980°C) Archaean regional metamorphism in the Napier Complex. J. Metamorph. Geol., **5**, 341–356.

HARLEY, S.L. (1998): On the occurrence and characterization of ultrahigh-temperature crustal metamorphism. What Drives Metamorphism and Metamorphic Reactions? eds. by P.J. TRELOAR and P.J. O'BRIEN. London, Geol. Soc., 81–107 (Geol. Soc. London, Spec. Pub., **138**).

HARLEY, S.L. and BLACK, L.P. (1997): A revised Archaean chronology for the Napier Complex, Enderby Land, from SHRIMP ion-microprobe studies. Antarct. Sci., **9**, 74–91.

HARLEY, S.L. and HENSEN, B.J. (1990): Archaean and Proterozoic high-grade terranes of East Antarctica (40–80°E): A case study of diversity in granulite facies metamorphism. High-Temperature Metamorphism and Crustal Anatexis, ed. by J.R. ASHWORTH and M. BROWN. London, Unwin Hyman, 320–370.

HENSEN, B.J. and MOTOYOSHI, Y. (1992): Osumilite-producing reactions in high temperature granulites from the Napier Complex, East Antarctica: Tectonic implications. Recent Progress in Antarctic Earth Science, ed. by Y. YOSHIDA *et al.* Tokyo, Terra Sci. Publ., 87–92.

HOKADA, T., ISHIKAWA, M, ISHIZUKA, H., OSANAI, Y. and SUZUKI, S. (1999): Alkali feldspar compositions of the Archaean Napier Complex, East Antarctica: Further evidence for 1100°C ultrahigh-temperature crustal metamorphism. Abst. 8th Int. Symp. Antarct. Earth Sci., Wellington (New Zealand), 144.

ISHIZUKA, H., ISHIKAWA, M., HOKADA, T. and SUZUKI, S. (1998): Geology of the Mt. Riiser-Larsen area of the Napier Complex, Enderby Land, East Antarctica. Polar Geosci., **11**, 154–171.

MAKIMOTO, H., ASAMI, M. and GREW, H.S. (1989): Some geological observations on the Archaean Napier Complex at Mt. Riiser-Larsen, Amundsen Bay, Enderby Land. Proc. NIPR Symp. Antarct. Geosci., **3**, 128–141.

MOTOYOSHI, Y. and HENSEN, B.J. (1989): Sapphirine-quartz-orthopyroxene symplectites after cordierite in the Archaean Napier Complex, Antarctica: Evidence for a counterclockwise *P-T* path ? Eur. J. Mineral., **1**, 467–471.

MOTOYOSHI, Y. and MATSUEDA, H. (1984): Archaean granulites from Mt. Riiser-Larsen in Enderby Land, East Antarctica. Mem. Natl Inst. Polar Res., Spec. Issue, **33**, 103–125.

OSANAI, Y., TOYOSHIMA, T., OWADA, M., TSUNOGAE, T., HOKADA, T. and CROWE, W.A. (1999): Geology of ultrahigh-temperature metamorphic rocks from the Tonagh Island in the Napier Complex, East Antarctica. Polar Geosci., **12**, 1–28.

SANDIFORD, M. (1985): The metamorphic evolution of granulites at Fyfe Hills; implications for Archaean crustal thickness in Enderby Land, Antarctica. J. Metamorph. Geol., **3**, 155–178.

SANDIFORD, M. and POWELL, R. (1986): Pyroxene exsolution in granulites from Fyfe Hills, Enderby Land, Antarctica: Evidence for 1000°C metamorphic temperatures in Archaean continental crust. Am. Mineral., **71**, 946–954.

SANDIFORD, M. and POWELL, R. (1988): Pyroxene exsolution in granulites from Fyfe Hills, Enderby Land, Antarctica: Evidence for 1000°C metamorphic temperatures in Archaean continental crust—Reply. Am. Mineral., **73**, 434–438.

SHERATON, J.W., OFFE, L.A., TINGEY, R.J. and ELLIS, D.J. (1980): Enderby Land, Antarctica—unusual Precambrian high-grade metamorphic terrain. J. Geol. Soc. Aust., **27**, 1–18.

SHERATON, J.W., TINGEY, R.J., BLACK, L.P., OFFE, L.A. and ELLIS, D.J. (1987): Geology of Enderby Land and Western Kemp Land, Antarctica. Aust. Bur. Mineral. Resour. Bull., **223**, 51p.

SPEAR, F.S. (1993): Metamorphic Phase Equilibria and Pressure-Temperature-Time Paths. Washington D.C., Mineral. Soc. Am., 799 p.

(Received March 15, 1999; Revised manuscript accepted May 14, 1999)